Published in Applied Physics Letters, 104, 081919 (2014). doi: 10.1063/1.4867017

Compressive deformation and failure of CrAlN/ Si_3N_4 nanocomposite coatings

S. Liu[1, 2], R. Raghavan[3], X.T. Zeng[2], J. Michler[3], W. J. Clegg[1]

[1]*Gordon Laboratory, Department of Materials Science and Metallurgy, 27 Charles Babbage Rd, Cambridge CB3 0FS, UK.*

[2]*Singapore Institute of Manufacturing Technology, 71 Nanyang Drive, Singapore 638075.*

[3]*Laboratory for Materials Technology, EMPA, Swiss Federal Laboratories for Materials Testing and Research, Feuerwerkerstr. 39, CH-3602 Thun, Switzerland.*

Abstract

The deformation and failure mechanisms of CrAlN/Si_3N_4 coatings containing grains a few nanometres in size have been compared with those of conventional CrN-based coatings. It is shown that the addition of amorphous Si_3N_4 phase increased the yield stress and hardness of the coating material, but did not change their ratio. This is consistent with theoretical predictions using existing models. However, cracking in conventional CrN-based coatings was catastrophic, whereas that in the fine-grained CrAlN/Si_3N_4 structure was much more benign, suggesting that the improved performance of these materials is associated with their fracture behaviours.

Hard coatings of nanometre-sized grains of a transition metal nitride, such as CrN, separated by an amorphous grain boundary film, such as Si_3N_4, show a greater resistance to erosion by particles[1], semi-dry wear in ball-on-disc tests[2], dry or semi-dry machining[1,3,4] and drilling[5] than conventional CrN-based hard coatings, particularly at higher speeds[4]. It has been suggested that this is associated with the greater hardness of these fine-grained coatings[2,4,6]. However, further understanding has been complicated by the lack of any direct measurements of the ratio of the hardness, H, to the uniaxial yield stress, Y.

In indentation, this is related to the ratio of the Y to the Young modulus E. Where Y/E is less than approximately 0.01, typical of metals, the material from the indent is pushed upward towards the surface, giving rise to pile-up, and the ratio of H/Y is equal to three[7]. However, for higher values of Y/E, such as might be expected in hard coatings, the material displaced from the indent is accommodated elastically in the sample below the plastic zone. In this case, the relationship between hardness and the yield stress can be determined by describing indentation in terms of an expanding cavity, which predicts that the ratio H/Y decreases with increasing Y/E[8,9]. However, in the materials with nanometre-sized grains it is thought that the high local pressures under the indent give rise to an increase in the elastic modulus[10]. Some calculations suggest that this might also cause an increase in the ratio of H/Y greater than would normally be expected and should be closer to three[11].

Recently, the microcompression test, originally developed for studying volume effects in metals[12], has been used to study deformation in hard materials, as the small sample size, of the order of 1 μm, suppresses cracking, allowing even the most brittle materials to be plastically deformed[13]. This enables the compressive yield stress, Y, to be directly measured, obviating the

need for calculation. The aim of this paper therefore is to establish the ratio of H/Y in CrN-based coatings experimentally and to investigate whether the differences in structure between the conventional CrN-based and the CrAlN/Si_3N_4 coatings change the way in which such materials deform.

The CrN, CrAlN and CrAlSiN coatings were deposited on Inconel 718 alloy substrates by a laterally rotating cathodic arc deposition system (Platit π^{80}, Switzerland) at bias voltage of –75 V and substrate temperature of 450 °C, described in detail elsewhere[14]. The as-deposited coatings were about 6 μm in thickness and were lightly polished to reduce the surface roughness.

The coating composition was determined by energy dispersive spectroscopy (Oxford Instrument, UK) on a scanning electron microscope (MX2600, CamScan) at an accelerating voltage of 12 kV. The crystal structure and chemical bonding states of the coatings were analysed by X-ray diffraction (Xpert, Philips) and X-ray photoelectron spectroscopy (ESCALab 250i-XL) respectively.

The internal stress in the coating was characterized by measuring the (422) peak shift in the XRD pattern at different angular off-sets[15]. The values of the internal stresses obtained are given in Table 1.

The hardness and Young modulus of the coatings were measured using a nanoindenter (Nanoindenter XP, MTS) with a Berkovich tip, using the continuous stiffness mode. To avoid substrate effects, the hardness was determined from indents whose depth was 450 nm, less than 0.1 of the coating thickness, and the Young modulus obtained by extrapolation to zero indent depth[16].

The micropillars of CrN, CrAlN and CrAlN/Si_3N_4 were made by focused ion beam milling (FIB) (Helios NanoLab 600, FEI Company, Netherlands). A high current Ga^+ ion beam (30 keV, 6.5 nA) was first used to mill a ring shaped trench with an outer diameter of 20 μm and inner diameter of 3.5 μm. The inner material was then milled at lower beam current (30 keV, 90 pA) to form a cylindrical pillar, followed by an even finer beam current (30 keV, 26 pA) to reduce the ion damage. Typically, the pillars had a height of about 800 nm, an aspect ratio of 2.5:1 and a taper of approximately 2°.

The micropillars were compressed using an *in situ* nanoindenter[17] with a 5 μm diameter diamond punch at a displacement rates of 5 nm^{-1}, and the stresses were obtained using the area of the top of the pillar where deformation was observed to start.

Before and after each compression, the micropillars were imaged using scanning electron microscope (Helios NanoLab 600) at a tilt angle of 52°, so that the sample deformation and failure modes could be studied. The compressed pillars were also examined by TEM (JEOL 2100), with the cross-sectional TEM samples prepared by FIB.

Table 1 summarizes the coating compositions studied together with their mechanical properties. Both the CrN and CrAlN coatings had columnar grain structures with average column widths of 230 nm and 130 nm respectively, Fig. 1a and 1b. The CrAlN grains were more elongated than the CrN grains. The CrAlN/Si_3N_4 coatings had equiaxed grains a few nanometers in size, Fig 1c. The X-ray diffraction (XRD) patterns showed that both the CrN and CrAlN coatings consist of rocksalt-structured crystallites, with (111) being the preferred out of plane orientation for both coatings. No Si related peaks were present in the X-ray diffraction patterns of CrAlN/Si_3N_4 coatings, suggesting the Si-containing phase was amphous. XPS analysis gave a binding energy

for the Si-2p of 101.2 eV, consistent with the formation of Si_3N_4. As Si has only a very low solubility in transition metal nitrides, the amorphous Si_3N_4 is likely to be present as a second phase with the CrAlN. TEM and SEM showed the presence of discrete particles of CrAlN, confirming the nanocomposite structure as consisting of particles of CrAlN in a matrix of amorphous Si_3N_4, consistent with that observed elsewhere.

The hardness of CrAlN was 30 GPa, substantially higher than that of the CrN coating, 19 GPa. The doping of Si into CrAlN increased the coating hardness to just over 32 GPa but reduced the internal stress almost by half, Table 1, although the CrAlN and CrAlN/Si_3N_4 coatings had similar Al/Cr atomic ratios.

Fig. 2a shows a typical stress-strain curve for a compressed CrAlN/Si_3N_4 micropillar. The pillar deformed elastically, before yielding at a stress of 16 GPa. Using the value of *E*, Table 1, this gives a value of *Y*/*E* of 0.04.

The material from which the pillar was milled contained in-plane residual stresses. The effect of these residual stresses would be to increase the measured yield stress, *Y*, of the coating, Table 1, to a value given approximately by[18]

$$Y = \sigma_Y + \sigma_R \qquad (1)$$

where σ_Y is the yield stress of the coating material in the absence of residual stresses and σ_R is the compressive residual stress, Table 1. Two bounds may be considered. The filled circle, Fig. 2b, represents the measured strength. If the residual stresses in the pillar have not relaxed, so that they have the value in Table 1, the yield strength of the material in the coating would be equal to the measured yield stress. If, as we might expect, the stresses have relaxed, then the

yield strength of the material as it is in the coating would be higher than the measured value, as given by Eqn. 1. This gives the lozenge in Fig. 2b.

Figure 2b also shows that the bounds of Y/E bracket the predictions from analyses where the material from the indent is accommodated mainly by the elastic compression of material underneath the indenter, as described by the expanding cavity model[9]. These analyses do not include effects associated with increased strain giving rise to increases in the elastic properties, and their agreement with the results here suggests that these effects are unimportant, at least, in the system here, despite the differences in structure.

On further compression, work hardening was observed. During this stage flow was localized in the upper region of the pillar, gradually spreading downwards. No cracking or shear band formation could be seen in the TEM, suggesting that deformation occurred by grain rearrangement, so that the grain boundary Si_3N_4 must be sufficiently soft under the test conditions to enable these materials to deform in a manner similar to a superplastic material. The hardness of the amorphous silicon nitride was measured as 18.8 GPa, slightly softer than the CrN.

In the CrN and CrAlN coatings failure was catastrophic, Fig. S1 (see supplemental material [19]), Fig. 3a and 3b. However, cracking in the CrAlN/Si_3N_4 occurred in a much more benign fashion, Fig. 3c. Cracks formed at the edge of the pillar, grew inward to the centre and down along the axis of the pillar, giving rise to a petal-like structure. High resolution SEM, Fig. 4a, and TEM, Fig. 4b, showed that the material failed intergranularly and suggested that deformation had occurred by grain rearrangement. The shape of the CrAlN grains in the nanocomposite was

clearly visible on the top surface and fracture cross-sections of the compressed pillar. They appeared intact and about 10 nm in size.

It is suggested that the more benign failure observed in the CrAlN/Si_3N_4 nanocomposite coating is associated with the development of the equiaxed structure caused by adding Si, so that failure along column boundaries, as has been observed in other coatings[20], is suppressed. Such an explanation would also be consistent with the increase in toughness that has been observed in the fine-grained coatings[21]. This increase occurs even though toughening by mechanisms such as crack-bridging would predict the reverse[22].

In summary, the deformation and failure of fine-grained CrAlN/Si_3N_4 coatings has been studied and compared with conventional CrN-based coatings. It has been shown that the formation of a fine-grained structure with each grain surrounded by amorphous Si_3N_4 phase enhances the yield stress of the coating material by approximately 40%, but does not change the flow field around an indentation, giving a value of H/Y of approximately 2, consistent with predictions in the literature. However, the nanocomposite structure appears to deform by the movement of grains with respect to one another, rather than by dislocation motion on macroscopic glide planes. This appears to suppress the growth of cracks by splitting.

This research was funded by A*STAR, Singapore and the Engineering and Physical Sciences Research Council (EPSRC) and Rolls-Royce Strategic Partnership “Structural Metallic Systems for Advanced Gas Turbine Applications” (EP/H500375/1). The authors also acknowledge Drs. X. Z. Ding, H. L. Seng, Z. Zhang, M. E. Vickers, Ms H. K. Hui and C.E. Davis for their technical assistance in this work.

Table

TABLE I. Composition, Young modulus, E, hardness, H, and internal stresses, σ_I, in the as-deposited CrN, CrAlN and CrAlN/Si_3N_4 coatings

Sample	Composition (at%)				Grain Size, nm	E, GPa	H, GPa	σ_I, GPa
	Cr	Al	Si	N				
CrN	49.7			49.7	230	310	19.2	3.8
CrAlN	18.9	31.9		48.9	130	440	30.2	7.3
CrAlSiN	16.6	28.3	3.4	51.3	10	380	32.5	4.1

References

[1] X. Z. Ding, X. T. Zeng, Y. C. Liu, Q. Yang, and L. R. Zhao, J. Vac. Sci. Technol., A **22** (6), 2351 (2004).

[2] M. Benkahoul, P. Robin, L. Martinu, and J. E. Klemberg-Sapieha, Surf. Coat. Technol. **203** (8), 934 (2009).

[3] C. Kim, M. C. Kang, J. S. Kim, K. H. Kim, B. S. Shin, and T. J. Je, Current Applied Physics **9** (1, Supplement), S145 (2009); Y. Tanaka, N. Ichimiya, Y. Onishi, and Y. Yamada, Surf. Coat. Technol. **146-147**, 215 (2001).

[4] P. Holubář, M. Jílek, and M. Šíma, Surf. Coat. Technol. **120-21**, 184 (1999).

[5] C. H. Zhang, X. C. Lu, H. Wang, J. B. Luo, Y. G. Shen, and K. Y. Li, Applied Surface Science **252** (18), 6141 (2006).

[6] Xing-zhao Ding, X. T. Zeng, and Y. C. Liu, Thin Solid Films **519** (6), 1894 (2011).

[7] R. Hill, E. H. Lee, and S. J. Tupper, Proc. Math. Phys. Eng. Sci. **188** (1013), 273 (1947).

[8] D. M. Marsh, Proc. Math. Phys. Eng. Sci. **279** (1378), 420 (1964); K. L. Johnson, Journal of the Mechanics and Physics of Solids **18** (2), 115 (1970).

[9] L.J. Vandeperre, F. Giuliani, and W.J. Clegg, J. Mater. Res. **19** (12), 3704 (2004).

[10] Stan Vepřek, Stephen G. Prilliman, and Simon M. Clark, J. Phys. Chem. Solids **71** (8), 1175 (2010).

[11] Maritza G. J. Veprek-Heijman, Ratko G. Veprek, Ali S. Argon, David M. Parks, and Stan Veprek, Surface and Coatings Technology **203** (22), 3385 (2009).

[12] Michael D. Uchic, Dennis M. Dimiduk, Jeffrey N. Florando, and William D. Nix, Science **305** (5686), 986 (2004).

[13] Johann Michler, Kilian Wasmer, Stephan Meier, Fredrik O□stlund, and Klaus Leifer, Appl. Phys. Lett. **90** (4), 043123 (2007); S. Korte and W. J. Clegg, Scr. Mater. **60** (9), 807 (2009).

[14] M. Jilek, T. Cselle, P. Holubar, M. Morstein, M.G J. Veprek-Heijman, and Stan Veprek, Plasma Chem Plasma Process **24** (4), 493 (2004).

[15] B. D. Cullity, *Elements of X-ray diffraction*, Third printing ed. (Addison-Wesley Publishing Co. Inc., 1967), p.514.

[16] N.M. Jennett, G. Aldrich-Smith, and A.S. Maxwell, J. Mater. Res. **19** (1), 143 (2004).

[17] J.M. Wheeler and J. Michler, Review of Scientific Instruments **84** (4), 045103 (2013).

[18] T. Y. Tsui, W. C. Oliver, and G. M. Pharr, J. Mater. Res. **11** (3), 752 (1996).

[19] See supplementary material at [URL] for stress-strain curves from the compression of CrN and CrAlN micropillars.

[20] J. M. Molina-Aldareguia, S. J. Lloyd, M. Odén, T. Joelsson, L. Hultman, and W. J. Clegg, Philos. Mag. A **82** (10), 1983 (2002).

[21] S. Liu, J.M. Wheeler, P.R. Howie, X.T. Zeng, J. Michler, and W.J. Clegg, Appl. Phys. Lett. **102** (17), 171907 (2013).

[22] Brian R. Lawn, *Fracture of Brittle Solids - Second Edition*, 2nd ed. (Cambridge University Press, Cambridge, 1993), p.p38.

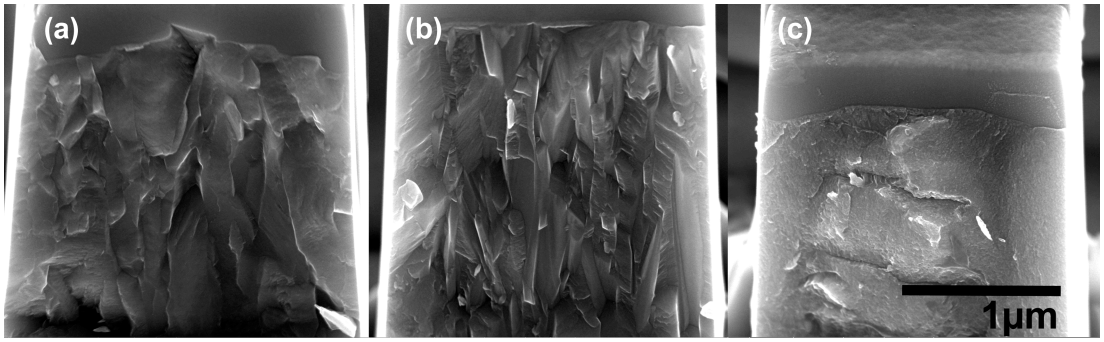

Fig.1 Fracture cross-sections of (a) CrN, (b) CrAlN and (c) CrAlN/Si_3N_4 coatings obtained by double cantilever beam compression[21] .

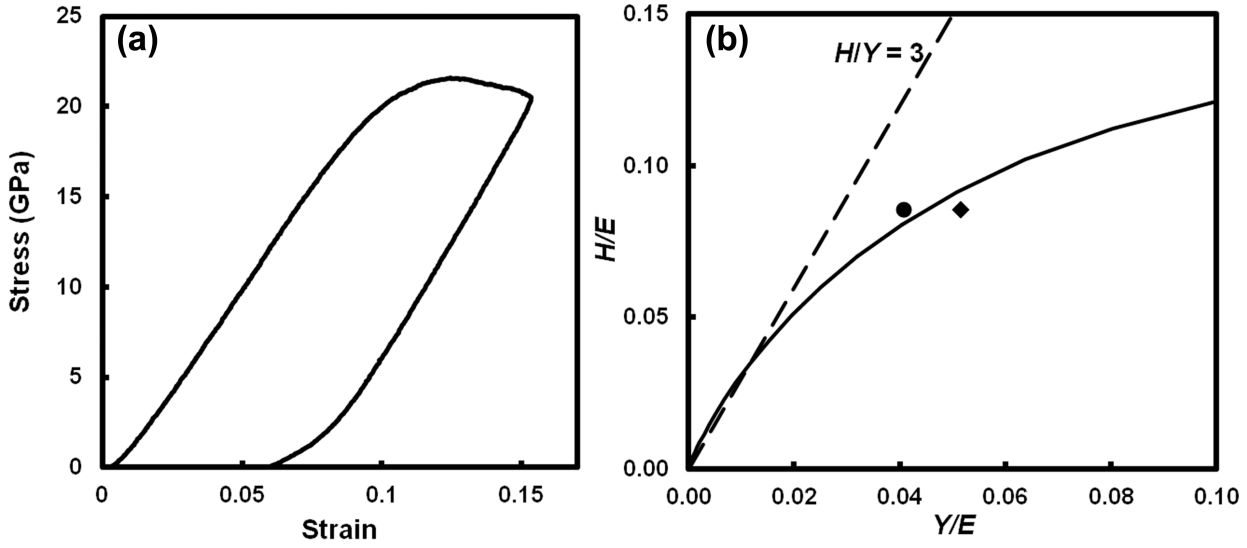

Fig. 2 (a) A typical stress-strain curve for CrAlN/Si_3N_4 micropillars, and (b) the variation of H/E with Y/E predicted by conventional models of indentation. The filled circle represents the measured value of Y/E, and the lozenge, what Y/E would be if the residual stresses had relaxed to zero in the micropillar.

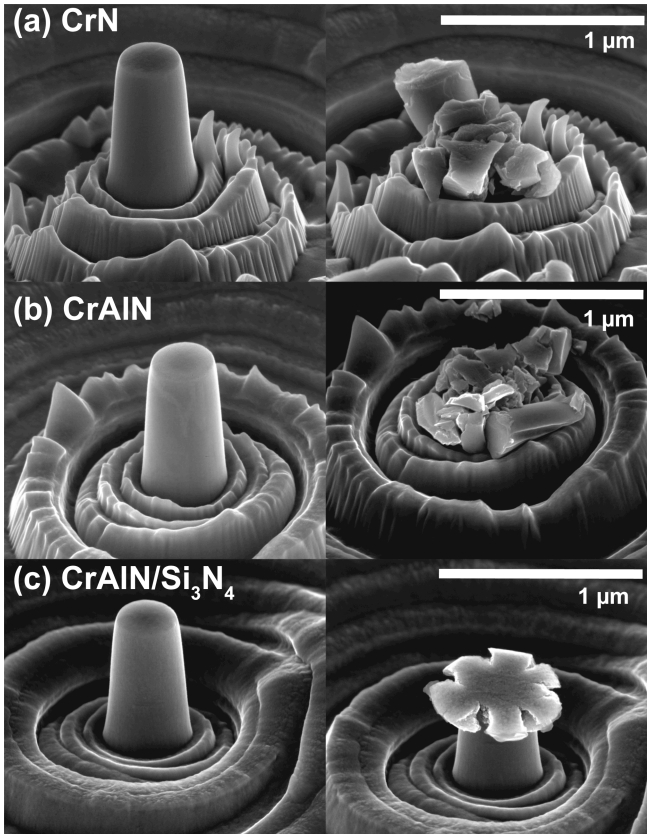

Fig. 3 SEM images showing original and compressed micropillars from (a) CrN, (b) CrAlN and (c) CrAlN/Si_3N_4 coatings.

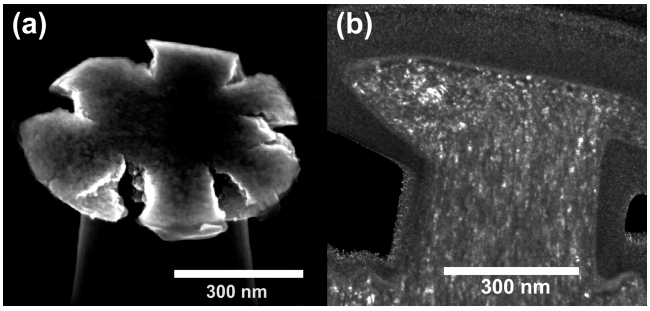

Fig. 4 High resolution (a) SEM and (b) dark field TEM images of compressed CrAlN/Si_3N_4 micropillars. In (a), the grains, approximately 10 nm in size in the nanocomposite structure can be seen, and in (b) that there are no apparent slip bands.